NTU Journal of Engineering and Technology (2026) 5 (1) : 84-96
DOI: https://doi.org/10.56286/ntujet.v5i1

IRAQI Academic Scientific Journals

P-ISSN: 2788-9971 E-ISSN: 2788-998X
NTU Journal of Engineering and Technology
Available online at: https://journals.ntu.edu.iq/index.php/NTU-JET/index

Design and Control Comparison of a SIMO DC–DC Converter for Electric Vehicle Applications

Faysal A. Jasim, Rakan Khalil ANTAR.
Northern Technical University, Technical Engineering College, Electrical Engineering Techniques, Mosul, Iraq
faysalhajjasim@ntu.edu.iq , rakan.antar@ntu.edu.iq

Article Informations

Received: 01-12- 2025,
Revised: 01-01- 2026,
Accepted: 09-01-2026,
Published online: 22-03-2026

Corresponding author:
Name: Faysal A. Jasim
Affiliation: Northern Technical University
Email:faysalhajjasim@ntue.edu.iq

Key Words:
DC-DC converter,
Single-Input Multi-Output,
sliding mode control,
electric vehicles,
efficiency improvement.

As electric vehicles become more widely used, there is a growing demand for more efficient and less complex power conversion technologies. Single-input, multi-output(SIMO) DC-DC converters are an essential component of electric vehicle voltage distribution systems, because it allows multi-level voltage supply from a single DC source such as a battery. Its importance is evident from the needs of the vehicle's various subsystems, including control units and auxiliary devices as well as the traction motor. This study deals with the design and analysis of a non-isolated single-input DC-DC converter (200V input) with three outputs: 400V, 24V, and 12V to provide voltage levels compatible with electric vehicle loads The proposed converter model is built and simulated in MATLAB/Simulink environment using a suitable topology combining one boost stage and two buck stages to provide a stable and highly efficient power supply to both the traction motor and auxiliary subsystems. To compare the dynamic and static performance, two control methods were implemented the first is sliding mode control (SMC) and the second is proportional integral control (PI. According to the obtained results, the SMC outperformed the PI controller in terms of voltage precision, disturbance rejection, reduced oscillations, and high efficiency exceeding 95%. This research work is strengthened by applying both PI and SMC control techniques in the design of a multi-output DC-DC converter within a simulation environment. The findings confirm the superiority of the SMC in maintaining regulated voltage and adjust to changes in load, making it the most suitable choice for electric vehicle.

1. Introduction

The polluted climate and the increasing use of fuels have led to the expanding use of electric vehicles (EVs), which become the basis of sustainable transportation [1,2]. The use of EVs enhanced transportation efficiency and reduced energy usage besides some problems such as high battery costs and charging time [3, 4].

In electric vehicles, the single-input, multi-output (SIMO) DC-DC converter is essential because it distributes power from the battery to the different subsystems, providing the proper voltages. Additionally, it supplies steady voltage to vital parts like the lighting systems, control units, and traction motor [5]. The converter transforms a single DC input into several reliable outputs that are tailored to each system's requirements while the driving vehicle [6]. As shown in Fig. 1, DC-DC converters are important for powering auxiliary systems and maintaining stable voltage across different loads. Relying on SIMO topology contributes to reducing system complexity, reducing cost and improving overall system efficiency [7, 8]. Typical batteries for electric vehicles usually run between 300 and 400 volts; in order to facilitate quicker charging and lower conduction losses, high-performance modern cars operate at a voltage of 800 volts [9]. Therefore, it is necessary to provide lower voltage levels to meet the requirements of auxiliary components, which requires voltage conversion to supply these components [10]. The purpose of DC-to-DC conversion in electric vehicles is to efficiently transfer electrical power from a high voltage source to multiple low voltage loads with low losses. Over the past decades, switching mode converters have gained wide popularity due to their versatility in stepping up, stepping down or inverting the DC voltage, Following the operating principle of converters mechanism in an AC system [11].

This research focuses on the design and performance implementation of a SIMO converter with a 200 V input and three different output voltages (400 V, 24 V, and 12 V). The converter model was simulated in the MATLAB/Simulink environment to evaluate its efficiency, verify voltage stability, and analyze ripple characteristics under various operating conditions. However, existing studies on SIMO DC–DC converters for electric vehicle applications mainly emphasize topological design or basic controller comparisons, with limited attention to the simultaneous regulation of multiple output voltages under varying load conditions. This work addresses this gap by presenting a focused control-oriented performance comparison, highlighting improved multi-output voltage regulation and dynamic response

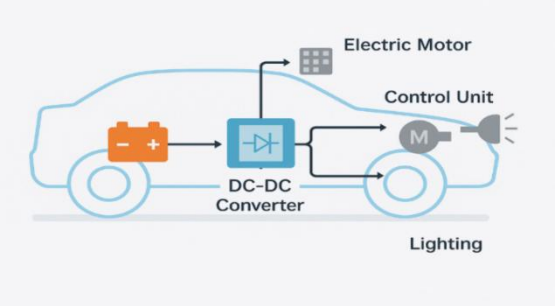

Fig. 1. Shows how the power of the proposed converter is distributed within the electric vehicle.

2. Related Work

Many researchers have focused on Improve performance DC–DC converter designs and control strategies for electric vehicle systems. Their work stresses the need to keep the output voltage stable and the efficiency high, even when the operating conditions change [12]. Although traditional PI controllers are widely used for their simplicity, they face challenges in handling sudden load changes and fast transients [13]. Sliding Mode Control (SMC), on the other hand, is a nonlinear control technique that has been introduced in recent research and has shown superior robustness and disturbance rejection capabilities [14]. Most of these studies have concentrated on isolated or single-output converters, with limited given to non-isolated SIMO topologies specifically designed to meet the diverse load requirements in electric vehicles. To fill this research void, the present work proposes the design and analysis of a non-isolated SIMO DC-DC converter with three outputs, applying SMC and PI controllers for comparative evaluation in a MATLAB/Simulink environment. Several topologies have been considered in these studies, and the following is some of the most relevant research in this field.

Sreeshma and Saradagi [15] provided a non-isolated SIMO DC-DC converter combining Zeta and Buck–Boost functions to provide multiple voltages. The model utilized state-feedback control with nonlinear compensation, achieving high efficiency and reduced switching losses. Nevertheless, the study highlighted response delays and steady-state errors under unparalleled disruptions.

Injeti and Das [16] suggested a DC-DC converter that is Single-Input Triple-Output using a single switch and coupled inductor. Voltage clamping and Zero Current Switching (ZCS) techniques were applied to achieve steady regulation with a 96.5% efficiency rate by minimizing switching losses and recycling leakage energy.

Sriram and Kumar [17] suggested a SIMO DC-DC converter that reduces switching losses by employing a switched-inductor structure with clamping diodes and ZCS techniques. The single-switch design achieved 96.3% efficiency and

generated three independent outputs with enhanced dynamic response. Considering output interdependence, control complexity stayed to be a problem.

According to Khaled A. Mahfuzah and Ali Q. Al-Shetwi [18] A hybrid Flyback-Cuk converter with two outputs was created that can operate efficiently at duty cycles close to 85% and achieve an overall efficiency of almost 89%..The system's appropriateness for application in EVs chargers, storage devices, and renewable energy interfaces is increased by its reliance on a single power switch, which results in reduced switching losses and fewer components.

Praveenkumar Chandran and Kaliamoorthy Mylsamy [19] designed a simple dual-output SIMO converter used to drive BLDC motors. Their design relied on only two switches, which helped accomplish about 96% efficiency keeping the torque constant and the output stable even when the input or load changed. The converter showed good potential for additional purposes such as LED lighting, and auxiliary units in electric vehicles

It is evident from the review above that the majority of current topologies have problems with complexity, cross-regulation, or output flexibility. Table (1) offers an analytical comparison of the technological variations and aids in determining the best options for EVs applications.

3. Proposed SIMO Dc-Dc Converter Topology

This section discusses the circuit topology and analytical characterization of the proposed non-isolated SIMO DC-DC converter. Electric vehicle traction motor drives and auxiliary subsystems require three regulated outputs of 400 V, 24 V, and 12 V, which the system is designed to generate with a single 200 V DC input. By giving a thorough explanation of power flow, operating modes, and mathematical control linkages, the analysis demonstrates how well the converter meets the demands of different loads in electric vehicle systems. Fig. 2 illustrates the distribution of power to the loads specific to the electric vehicle.

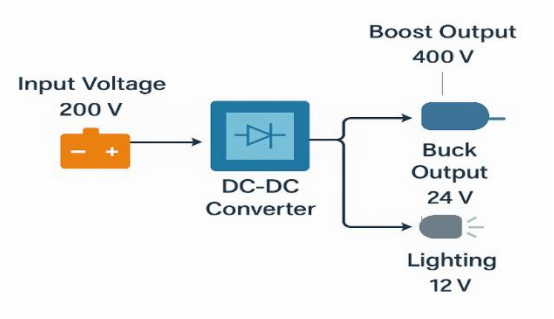

Fig. 2. A diagram of the proposed SIMO DC-DC converter.

3.1 Case 1: Proposed First Topology

The first proposed model of the designed SIMO DC-DC converter builds with a structure of one input (200V) and three-outputs depending on one inductor. The first output is boosting the input to 400V and the other outputs designed to give 12V and 24V.

The designed topology offers different levels of DC voltage levels required for EVs. The power circuit gives 400V DC output to drive the EV's motor, and 24V and 12V DC to support loads and control units that need these low DC voltages. One inductor shared among all outputs with output capacitors and diodes to ensure voltage regulation under steady-state operating conditions are the main elements of the proposed SIMO circuit. A PI controller is implemented to adjust these output voltages. The PI parameters were adjusted to accomplish a cooperation between fast transient and stable steady-state acts with lower steady-state voltage errors. Modelling outcomes confirmed that the recommended SIMO accomplished stable outputs with an efficiency of 97.09%.

Table 1. Comparative analysis of various DC–DC converter configurations used in electric vehicle systems

Ref. No	Efficiency	Number of Switches	Number of Capacitors	Number of Inductors	Number of Outputs	Input Voltage	Output Voltage
[15]	---	1	3	2	2	9v	12v,5v
[16]	96.5%.	1	5	3	3	12v	200v,30v,40v
[17]	96.3%	1	4	2	2	12v	24v,48v
[18]	89%	1	3	2	2	220v	50v, -24v
[19]	96.16%	2	3	2	2	12v	72.6v,5.2v
Proposed SIMO	Case I = 97.090%	3	3	1	3	200v	400v,24v,12v
	Case II= 99%	3	3	3	3	200v	400v,24v,12v

Figure 3 illustrates the power-stage configuration of the SIMO DC–DC converter, where a single shared inductor is used to feed one boost stage and two buck stages. The boost path supplies the high-voltage output for the traction motor, while the buck paths provide regulated low-voltage outputs for auxiliary loads. The figure also highlights the placement of the power switches, diodes, and output capacitors, which together enable independent voltage regulation through the PI control loops..

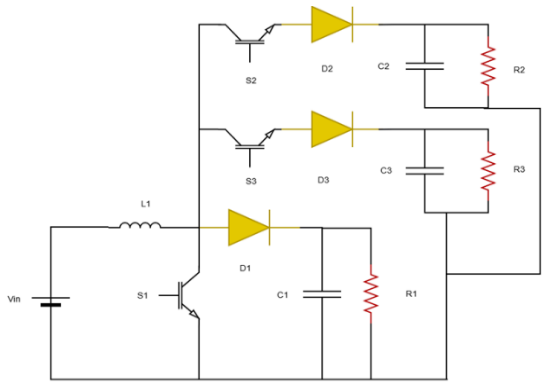

Fig. 3. Circuit topology of the proposed first SIMO DC-DC converter with PI controller.

3.1.1. Modes of operation

The operation of the proposed first SIMO DC–DC converter can be divided into different switching states depending on the ON/OFF condition of the power switches. Each switch is associated with one of the three regulated outputs (400 V, 24 V, and 12 V). The output voltage of the Boost stage due to switch S1 is given by:

$$V_{o1} = \frac{V_{in}}{1 - D_1}$$

This equation was derived in the following way:

Mode1
Assuming that the inductor current rises linearly from I1 to I2 in time t1

$$V_{in} = L1\left(\frac{I_2 - I_1}{t_1}\right) \quad (1)$$

And

$$t_1 = \frac{\Delta I\, L}{V_{in}} \quad (2)$$

Mode2
The inductor current falls linearly from I2 to I1 in time t2

$$V_{in} - V_{o1} = -L1\frac{\Delta I}{t_2} \quad (3)$$

$$t_2 = \frac{\Delta I\, L}{V_a - V_s} \quad (4)$$

$$\Delta I = \frac{V_{in} t_1}{L1} = \frac{(V_{o1} - V_{in})\, t_2}{L1} \quad (5)$$

$$V_{o1} = V_{in}\frac{T}{t_2} \quad (6)$$

$$\because \ \frac{T}{t_2} = D_1 \quad (7)$$

$$\therefore \ V_{o1} = \frac{V_{in}}{1 - D_1} \quad (8)$$

Equation No. (7) represents the first output voltage of the system while S2 and S3 will be responsible for the buck stages and the outputs are calculated as

$$V_{o2} = D_2 \cdot V_{in} \quad \text{(output2)}$$
$$V_{o3} = D_3 \cdot V_{in} \quad \text{(output3)}$$

For brevity, the mathematical derivation is provided only for the second output stage, as the third output stage operates under the same principle and follows similar derivation steps
Mode 1 (Switch ON)
During t1, the inductor current increases linearly

$$V_{in} - V_{o2} = L2\frac{I_2 - I_1}{t_1} = L2\frac{\Delta I}{t_1} \quad (9)$$

$$t_1 = \frac{\Delta I\, L}{V_{in} - V_{o2}} \quad (10)$$

Mode 2 (Switch OFF)
During Mode 2, the inductor current decreases linearly from I_2to I_1over the interval t_2, as the energy stored in the inductor is delivered to the output through the freewheeling diode.

$$-V_{o2} = -L2\frac{\Delta I}{t_2} \quad (11)$$

t2 : OFF time interval of the switch

$$t_2 = \frac{\Delta I\, L}{V_{o2}} \quad (12)$$

$$\Delta I = \frac{(V_{in} - V_{o2})t_1}{L2} = \frac{V_{o2} t_2}{L2} \quad (13)$$

Substituting $t_1 = D_2 T$ and $t_2 = (1 - D_2)\, T$ yields the average output voltage as:

$$V_{o2} = V_{in}\frac{t_1}{T} \quad (14)$$

$$\because \ D_2 = \frac{t_1}{T} \quad (15)$$

$$\therefore \ V_{o2} = D_2 V_{in} \quad (16)$$

Equation No. (16) represents the second output voltage in the system.

3.1.2 Control Strategy

To regulate the three output voltages of the proposed first SIMO converter, a conventional Proportional–Integral (PI) control strategy is implemented. Independent feedback loops are designed for each output so that the duty cycle of each switch is adjusted according to the voltage error. The control law is expressed as:

$$e_i(t) = V_{ref,i} - V_{o,i}(t) \quad (17)$$

where $i \in \{1,2,3\}$

The continuous-time PI regulator is defined as [20]:

$$u_i(t) = K_{p,i}\, e_i(t) + K_{i,i} \int e_i(t)\, dt \quad (5)$$

The controller output is translated into a duty ratio command, limited between 0 and 1:

$$D_i(t) = \text{sat}\left(g_i\left(u_i(t)\right)\right), \quad 0 \le D_i \le 1 \quad (18)$$

Where Di(t) is duty ratio of the *i-th* switch at time t, ui(t) is the control input signal generated by the controller, gi(·) is mapping function that transforms the control signal into a normalized form, and sat(·) is saturation function ensuring the duty ratio remains within the range [0,1].

For digital implementation with sampling time Ts, the discrete incremental form is [20]:

$$u_i[k] = u_i[k-1] + K_{p,i}\,(e_i[k] - e_i[k-1]) + K_{i,i}\,T_s\,e_i[k] \quad (19)$$

The tuning of KP_i ,Ki_i was performed considering the averaged converter relations, with the objective of achieving fast dynamic response, minimal overshoot, and zero steady-state error. An iterative trial-and-error procedure was applied under different load conditions, and the selected gains were validated through time-domain simulations.

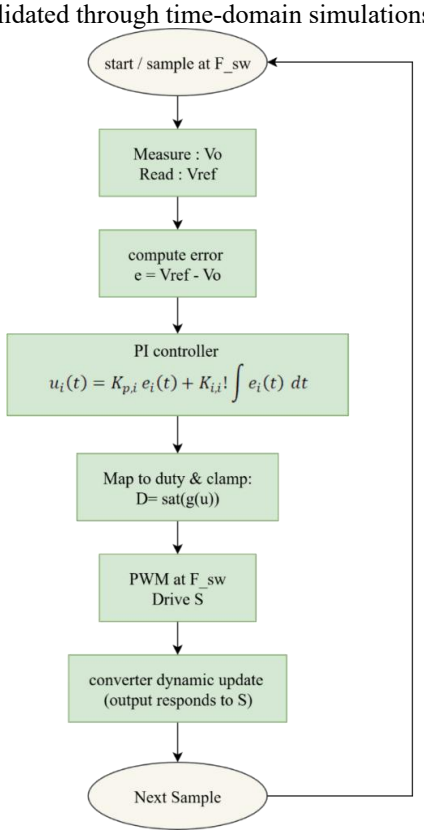

Fig. 4. Flowchart of the PI control strategy for the proposed first SIMO DC-DC converter.

The complete flowchart of the PI control algorithm for the three outputs is illustrated in Fig. 4, which summarizes the process of error calculation, PI regulation, duty update, and PWM generation.

3.1.3 Simulation Setup

The proposed first topology of SIMO DC–DC converter with PI control was implemented and analyzed by MATLAB/Simulink. Table 2 shows the the system parameters of the proposed SIMO DC–DC converter under PI control.

Table 2. Simulation parameters of the proposed SIMO DC–DC converter

Parameter	Symbol	Value	Description
Input voltage	V_{in}	200v	DC source
Traction motor	V_{o1}	400v	Output voltage 1 (Boost)
Auxiliary load	V_{o2}	24v	Output voltage 2 (Buck 1)
Control unit	v_{03}	12v	Output voltage 3 (Buck 2)
All switches Inductor	*swf*	20KHZ	Switching frequency Shared inductor
Inductor	L	2mH	Shared inductor
Capacitor (Boost)	C1	1000 µf	Output filter
Capacitor (Buck 1)	C2	1000 µf	Output filter
Capacitor (Buck 2)	C3	1000 µf	Output filter
Load resistance	R1	20 Ω	Boost load
Load resistance	R2	2 Ω	Buck 1 load
Load resistance	R3	1.2 Ω	Buck 2 load
Integral gain &Proportional gain	K_p & K_i	0.3401 & 40	Tuned values (Boost)
Integral gain &Proportional gain	K_p & K_i	0.2648 & 0.4333	Tuned values (Buck 1)
Integral gain &Proportional gain	K_p & K_i	0.648 & 1.4	Tuned values (Buck 2)

3.1.4 Results and performance discussion

The proposed first SIMO DC–DC converter controlled by the PI regulator was simulated and analyzed using MATLAB/Simulink. The voltage response results of the three output voltages (400 V, 24 V, and 12 V) are shown in Fig. 6. The results demonstrate that all output voltages reached their reference values with a smooth transient response and without significant oscillations or overshoot.

It can be observed that the figure illustrates the output voltage waveforms for the three voltage levels. The overshoot remains very small and well limited for all outputs, while both the rise time and settling time are short, with no noticeable oscillations during the transition to steady-state operation The system achieved a rapid rise time and short settling period, indicating good dynamic behavior of the converter using the designed PI controller.

The converter also exhibited high efficiency, maintaining an average value of approximately 97.090**%**, which validates the effectiveness of the single-inductor SIMO configuration in reducing power losses. Table 3 summarizes the performance metrics, efficiency, and other general parameters, and confirms that the proposed converter provides multiple outputs suitable for electric vehicle applications.

Table 3. Simulation parameters of the proposed SIMO DC–DC converter.

Output voltage	Rise Time (µsec)	Over shoot (%)	Settling Time(sec)	Steady state error	(η)
400	45	26.53	0.000556	12.0083	97.1
24	32	6.72	0.031467	0.0006	
12	29	16.98	0.032764	0.0029	

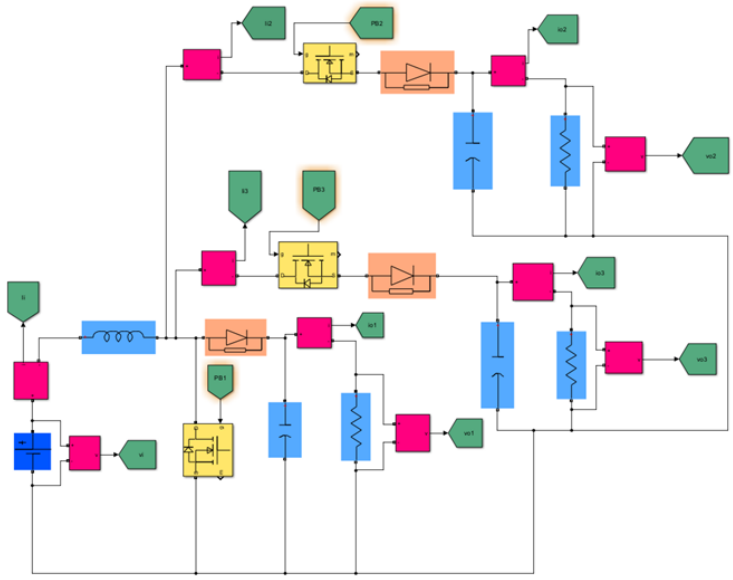

Fig. 5. MATLAB/Simulink model of the proposed SIMO DC–DC converter under PI control: (Power stage).

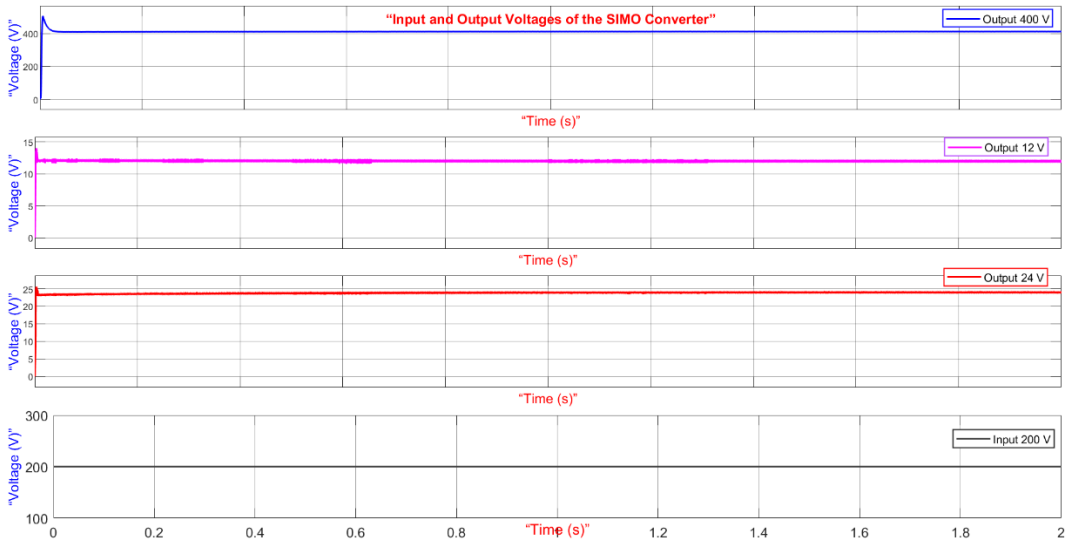

Fig . 6. Output and input voltage waveforms of the proposed SIMO DC-DC converter under PI control.

3.2 Case 2: Proposed Second Topology

In the second configuration, the proposed second SIMO DC–DC converter keeps structure of Boost–Buck–Buck topology but employs independent inductors (L_1, L_2, and L_3) for each output stage. This design delivers three regulated voltages of 400 V, 24 V, and 12 V from a single 200 V DC input In contrast to the PI-controlled structure used in Case 1, this configuration adopts a Sliding Mode Control (SMC) strategy to improve robustness against load variations and parameter uncertainties. To evaluate the effect of different SMC formulations on system behavior, three controller variants were implemented and tested:

1. Classical SMC (CSMC) — based on the error and its derivative.
2. Integral SMC (ISMC) — includes the error integral to remove steady-state deviation.
3. Adaptive SMC (ASMC) — adjusts the control gain adaptively for improved dynamic behavior.

The proposed second converter and controller schemes were modeled and simulated as illustrated in Fig. 7.

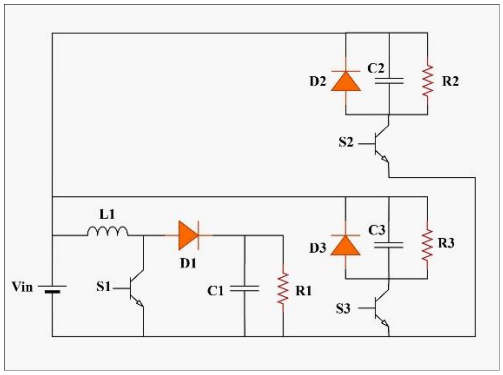

Fig . 7. Circuit topology of the proposed second SIMO DC-DC converter using Sliding Mode Control technique.

3.2.1. Modes of operation

The proposed second SIMO DC–DC converter circuit is operating based on SMC function through two fundamental switching intervals for each output branch. Switches S1, S2, and S3 regulate one of the three output voltages (400 V, 24 V, and 12 V, respectively) depending on derived one input DC voltage of 200V.The capacitors C1, C2, and C3 play a crucial role in energy storage and voltage filtering, maintaining output voltage stable and reducing ripple during high-frequency switching transitions [21].

The SMC ensures that the system trajectory is constrained to the predefined sliding surface, resulting in enhanced robustness and fast dynamic performance under load or input disturbances [21].

3.2.2 Control strategy

The SMC method was applied in the projected second SIMO DC–DC converter circuit to overwhelm the restrictions of the conventional PI controller, which displayed overshoot, sluggish transient response, and slight oscillations during load variations. The SMC method confirms a fast dynamic response, high strength against disturbances, and higher flexibility. In this type of nonlinear controller, the switching mechanism successfully decreases voltage overshoot and oscillations, resulting in a smoother output related to linear controllers. This means that SMC is specifically suited for EV requests where stable voltage and fast load fluctuations are important [22].

The control is made from of three main components: the error signal, the sliding surface, and the control law. The instantaneous voltage error between the reference and measured output is described as [23]:

$$e_i(t) = V_{ref,i} - V_{o,i}(t) \tag{20}$$

Where Vref, i is reference voltage of output (i=1, 2, 3), and Vo,i(t) is actual output voltage at time *t*. Also, The sliding surface determines the desired system dynamics and ensures that the trajectory converges smoothly toward equilibrium [23].

$$s_i(t) = \frac{de_i(t)}{dt} + \lambda_i e_i(t) \tag{21}$$

Where λi is a positive constant determining the slope of convergence, and $s_i(t)$ is sliding surface of the output. The control signal is generated based on the sign of the sliding surface.

$$u_i(t) = K_i \,\mathrm{sgn}\big(s_i(t)\big) \tag{22}$$

where ui(t) is control signal or duty ratio for the output, Ki is control gain, and sign (·) is signum function which is defined as:

$$sgn(s_i) = \begin{cases} -1, & s_i < 0 \\ +1, & s_i > 0 \end{cases} \tag{23}$$

To improve performance even more SMC variants (Classic, integral, adaptive) were implemented and tested in the proposed converter To increase convergence speed, each variation alters the control gain or sliding surface. eliminate steady-state error, and adapt to load variations. The control signal generated from each SMC loop is converted into a PWM duty ratio that drives the power switches S1, S2, and S3. Collectively, these techniques demonstrate superior voltage stability and reduced overshoot compared to PI control, confirming the suitability of SMC-based regulation for multi-output electric vehicle converters. The sliding mode control parameters were selected based on the averaged converter model and refined using an iterative trial-

and-error approach. The sliding surface slope λ_i was chosen to ensure fast error convergence, while the control gain K_i was adjusted to achieve robust voltage regulation under load variations without introducing excessive chattering. The final parameter values were validated through simulation by evaluating transient response and voltage regulation performance.

Figure 8 presents a flowchart illustrating the dynamic behavior of the sliding mode control strategy, showing the error computation, sliding surface generation, and control law formulation.

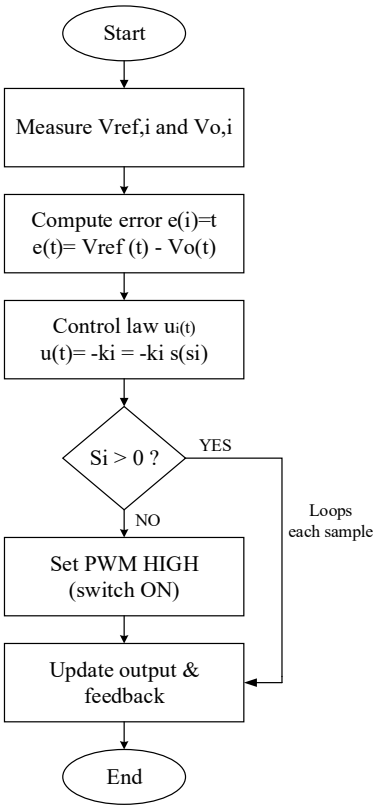

(a)

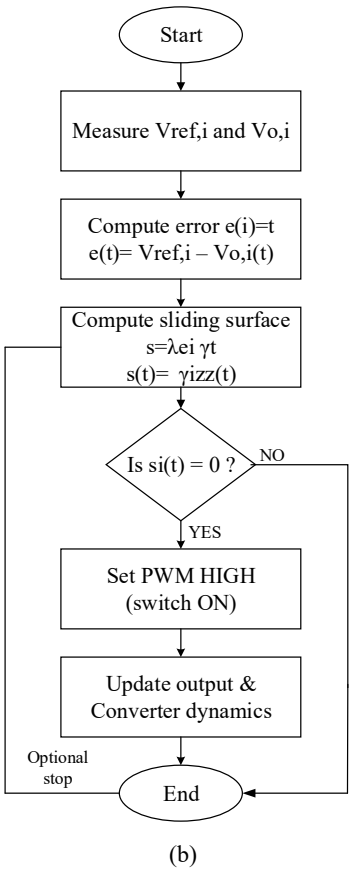

(b)

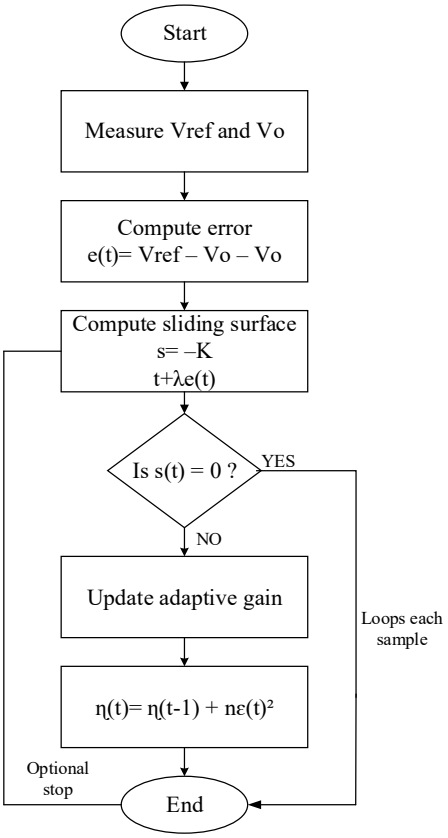

(c)

Fig . 8. Flowcharts of the proposed SMC-based control strategies: (a) Classical SMC, (b) Integral SMC, (c) Adaptive SMC.

3.2.3 Simulation Setup

The proposed second SIMO DC–DC converter shown in Fig. 7 with SMC was modeled and simulated by MATLAB/Simulink. The same converter parameters used in the first SIMO circuit case were maintained to ensure a fair performance comparison. However, Classical Sliding Mode Control (CSMC), Integral Sliding Mode Control (ISMC), and Adaptive Sliding Mode Control (ASMC) were tuned to achieve optimal voltage regulation and fast transient response. The main circuit parameters and control constants employed in the simulation are summarized in Table 4.

Table 4. Simulation parameters and control constants used for the proposed second SIMO DC–DC converter under (SMC technique).

Parameter	Symbol	Value	Description
Input voltage	V_{in}	200v	DC source
Traction motor	V_{o1}	400v	Output voltage 1 (Boost)
Auxiliary load	V_{o2}	24v	Output voltage 2 (Buck 1)
Control unit	V_{03}	12v	Output voltage 3 (Buck 2)
Inductor	L1, L2, L3	1mH	Enrgy storage inductors
Capacitor (Boost)	C1	1000 µf	Output filter
Capacitor (Buck 1)	C2	500 µf	Output filter
Capacitor (Buck 2)	C3	1000 µf	Output filter
Load resistance	R1	20 Ω	Boost load
Load resistance	R2	16 Ω	Buck 1 load
Load resistance	R3	16 Ω	Buck 2 load

Table 5 summarizes the control parameters used in the three types of SMC. The classical controller establishes the foundation of nonlinear control, the integral type enhances steady-state stability, and the adaptive version dynamically adjusts the control gain according to operating conditions. Fig. 9 illustrates the principal operation of the three SMC types.

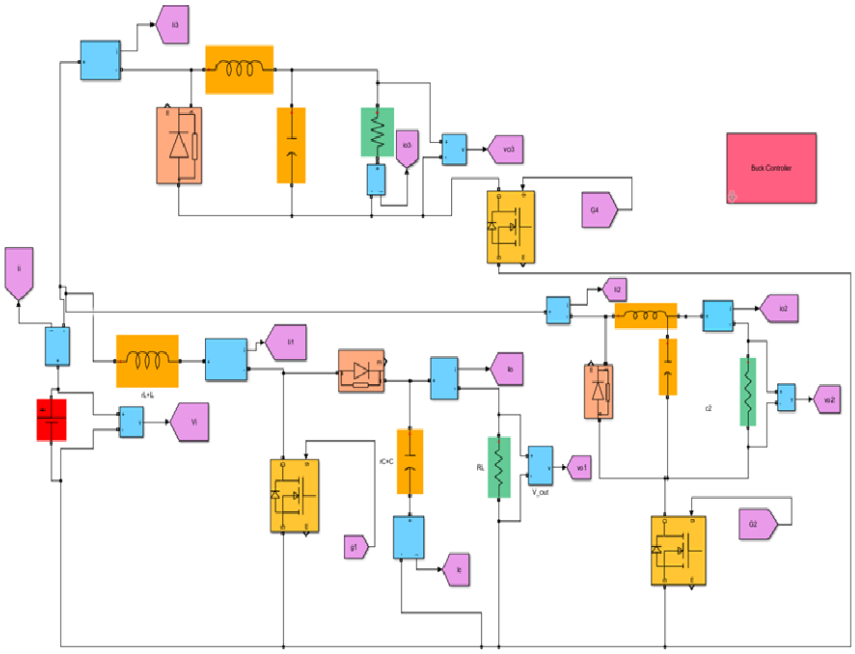

Fig. 9. MATLAB/Simulink model of the proposed Boost–Buck–Buck SIMO DC–DC converter under different Sliding Mode Control configurations

Table 5. Control parameters of the three SMC types.

Control Type	Parameter	Symbol	Value	Description
Classical SMC	Control Gain	Kp1 V_{o1} Kp1 V_{o2} Kp1 V_{o3}	142.7 1000 900	Determines the amplitude of switching action
	Secondary proportional gain (for switching or correction term)	Kp2 V_{o1}	2.7	Secondary gain to enhance switching response and convergence speed.
	Beta1	β1 V_{o1}	0.25	Switching response adjustment factor
	Beta2	β2 V_{o1}	0.25	Adaptive gain tuning factor
Integral SMC	Control Gain	Kp1 V_{o1} Kp1 V_{o2} Kp1 V_{o3}	415 4 4	Controls initial response speed of the SMC system.
	Negative gain block	-K / V_{o2} -K/ V_{o3}	0.002 0.002	inverting gain block used to reverse the sign of the derivative term
	Beta1	β1/ V_{o1}	0.25	Switching response adjustment factor
	Beta2	β2 / V_{o1}	0.25	Adaptive gain tuning factor
	Adaptive Gain Constant	Ka	125	Fixed gain for adaptive control tuning and switching stability.
Adaptive SMC	Switching Frequency	Swf	100kHz	Switching frequency for all converters
	Lambda for Current (Boost)	λ_i	300	Sliding surface coefficient related to inductor current dynamics
	Lambda for Voltage (Boost)	λ_v	90	Sliding surface coefficient related to output voltage dynamics
	Eta (Boost)	η	50	Adaptive control coefficient determining switching intensity
	Gamma (Buck 1) Gamma (Buck 2)	γ_2 γ_3	0.01 0.01	Adjustment gain for converter

3.2.4 Results and performance discussion

Figure 10 presents the output voltages of the proposed second SIMO DC–DC converter under three SMC strategies. All control methods successfully regulated the three output voltages (400 V, 24 V, and 12 V) from a single 200 V input source. It can be observed that the figure illustrates the output voltage waveforms corresponding to the three SMC approaches, namely Classical SMC, Integral SMC, and Adaptive SMC, as shown in subfigures (a), (b), and (c), respectively. The results indicate that all strategies achieve stable voltage regulation with small overshoot and smooth transient behavior. In particular, the adaptive SMC demonstrates improved transient response with reduced settling time compared to the other methods, while maintaining accurate voltage tracking for all output levels.

The CSMC achieved a fast transient response with minor ripples and an efficiency of 97.99%, whereas the ISMC demonstrated superior voltage stability and the highest efficiency of 99%, effectively eliminating steady-state error While ASMC maintained strong robustness to parameter variations with an efficiency of 97%, though it exhibited a slightly slower settling response.

According to the results obtained, the integral-type converter achieved notable excellence in voltage stability and high efficiency, making it a suitable choice for multi-output DC-DC converters used in electric vehicles. Table 6 displays the performance indicators for each control type, highlighting parameters which represent the steady-state error, voltage overshoot, rise time, and settling time, in addition to the system efficiency.

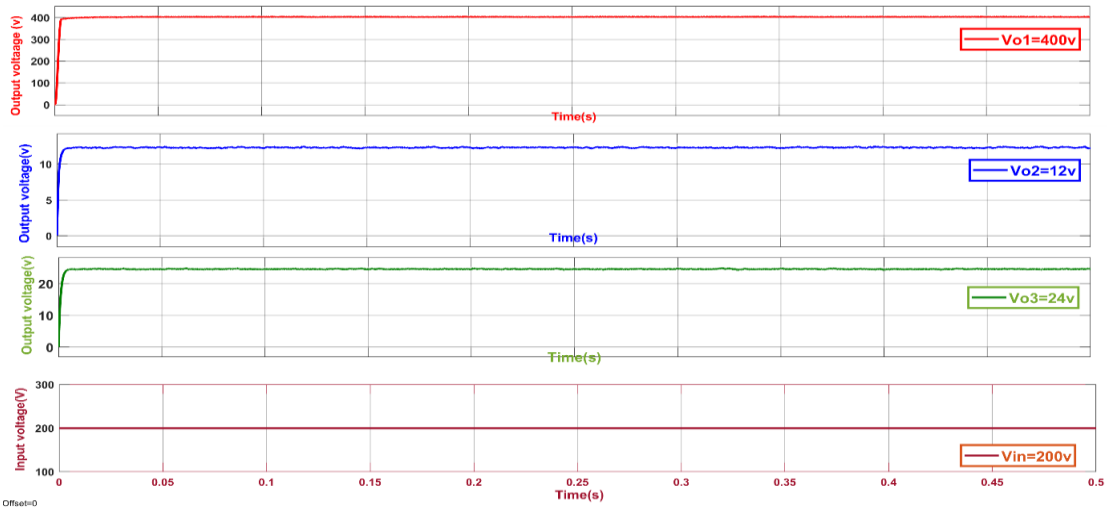

(a)

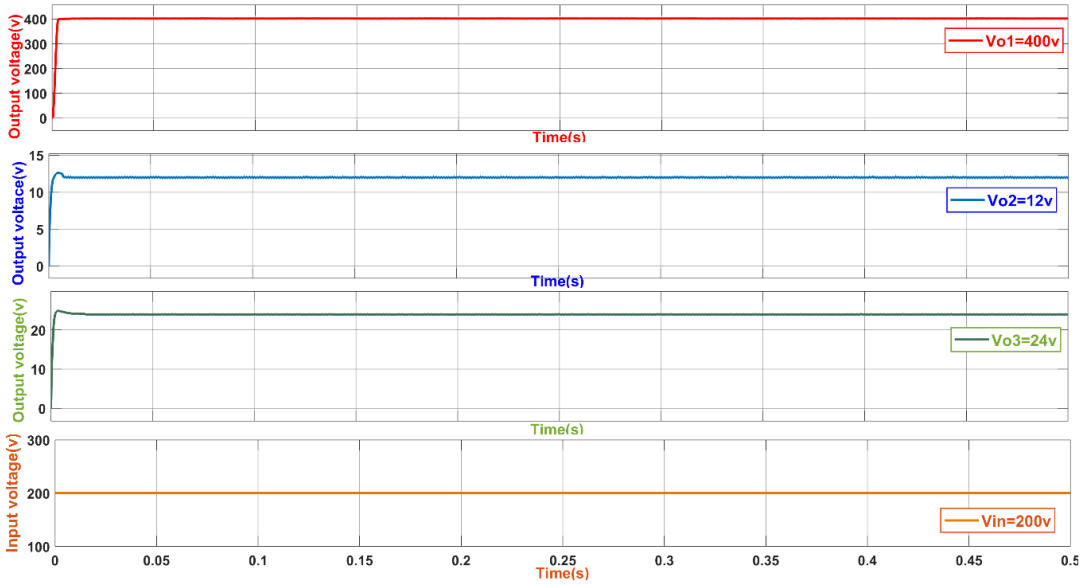

(b)

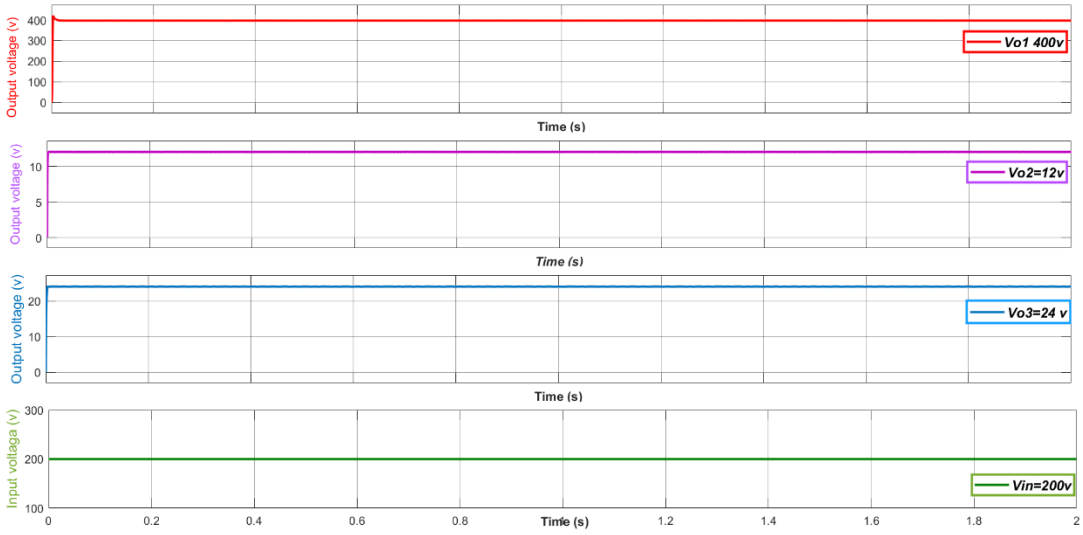

(c)

Fig. 10. Output and input voltage waveforms of the proposed SIMO DC–DC converter under (a) Classical SMC, (b) Integral SMC (c) Adaptive SMC.

Table 6. A comparison Performance parameter of the proposed converter under SMC controller for the three methods

control Type	Output Voltage (V)	Rise Time (µsec)	Overshoot (%)	Settling Time (µsec)	Steady-State Error (%)	Efficiency (η) (%)
Classical SMC	400	46	1.26	78	3.3587	98.621
	24	49	3.50	49972	0.4168	
	12	40	4.70	407700	0.4083	
Integral SMC	400	43	0.65	72	1.7291	99
	24	32	3.79	181	0.0360	
	12	36	5.22	172	0.0381	
Adaptive SMC	400	38	5.34	158	2.7493	96.716
	24	41	1.15	64	0.0805	
	12	33	0.98	46	0.0601	

4. Conclusion

This paper offers an investigation into the design and implementation of two types of SIMO DC-DC converters, designed based on as a Boost–Buck configuration and employed to the power distribution management of electric vehicles, An analysis was carried out on the operating principle of the proposed converter and its different modes of operation., with a focus on simple construction, high efficiency, and the ability to provide regulated power via multi-lEVsel output.

The first converter is designed using a conventional PI controller, while the second converter is designed using three-way slide control (conventional, integral, and adaptive) to provide three outputs (400V, 24V, and 12V) from a 200V DC supply. All the implemented control strategies succeeded in maintaining stable output regulation and reducing complexity, maintaining high power, and providing robustness against load changes however, the results indicated that the Sliding Mode Control (SMC), when applied to a multi-output converter, demonstrated outstanding performance. compared to conventional linear approaches.

It outperformed the Proportional-Integral (PI) controller in terms of transient response speed, voltage stability, steady state, and low ripple, achieving an overall efficiency of 99%. making it the most suitable choice for modern electric vehicle power systems.

Future work will focus on extending the simulation-based framework adopted in this study by integrating artificial intelligence techniques and optimization algorithms with sliding mode control to further enhance dynamic performance, efficiency, and robustness. Advanced simulation studies provide an effective means to evaluate system behavior under diverse operating conditions, offering a reliable foundation for the development of modern electric vehicle power systems.

References

[1] B. C. D. S. A. N. R. K. M. A. R. Venugopal1, "Review on Unidirectional Non-isolated High Gain DC-DC Converters for EV Sustainable DC Fast Charging Applications," 2021.

[2] B. Faridpak, M. Farrokhifar, S. Member, M. Nasiri, A. Alahyari, and N. Sadoogi, "Developing a Super-Lift Luo-Converter with Integration of Buck Converters for Electric Vehicle Applications."

[3] F. S. Abdulla, A. N. Hamoodi, and A. M. Kheder, "Particle Swarm Optimization Algorithm for Solar PV System under Partial Shading.," *Przeglad Elektrotechniczny*, vol. 97, no. 10, 2021.

[4] R. Islam, S. M. S. H. Rafin, and O. A. Mohammed, "Comprehensive Review of Power Electronic Converters in Electric Vehicle Applications," Mar. 01, 2023, *MDPI*. doi: 10.3390/forecast5010002.

[5] H. Javvaji, G. Madhavi, V. Harika, G. Veeranna, M. Khan Patan, and M. Hussain, "Single Input And Multiple Output DC-DC Converter For Electric Vehicle Applications", *J Theor Appl Inf Technol*, vol. 15, no. 11, 2023, [Online]. Available: www.jatit.org

[6] M. Dhananjaya, D. Potnuru, P. Manoharan, and H. H. Alhelou, "Design and Implementation of Single-Input-Multi-Output DC-DC Converter Topology for Auxiliary Power Modules of Electric Vehicle," *IEEE Access*, vol. 10, pp. 76975–76989, 2022, doi: 10.1109/ACCESS.2022.3192738.

[7] C. Vishnuvardhan and S. Wazeed, "A New Multi-Output DC-DC Converter for Electric Vehicle Application," *Journal of Energy Engineering and Thermodynamics*, no. 26, pp. 37–44, Nov. 2022, doi: 10.55529/jeet.26.37.44.

[8] R. K. Antar, A. A. Saleh, T. T. Yahia, "Estimate and Control speed of a DC motor using Different Power Circuits", Przegląd Elektrotechniczny Journal, Vol. 2023, No. 3, pp. 271-276, march 2023. http://doi:10.15199/48.2023.03.48. http://pe.org.pl/articles/2023/3/48.pdf

[9] S. Sankara Kumar and K. Ramash Kumar, "Design of Single Input Dual Output DC-DC Converter for Electric Vehicle Application," *Math Probl Eng*, vol. 2023, 2023, doi: 10.1155/2023/3536608.

[10] R. K. Antar, "Design and Analysis of A Sinusoidal PWM Rectifier Circuit Under Different Operating Conditions," *J Teknol*, vol. 87, no. 3, pp. 443–454, May 2025, doi: 10.11113/jurnalteknologi.v87.21586.

[11] C. Díaz-Martín, E. Durán, S. P. Litrán, J. L. Álvarez, and J. Semião, "Single-Switch Non-Isolated Resonant DC-DC Converter for Single-Input Dual-Output Applications," *Applied Sciences (Switzerland)*, vol. 13, no. 15, Aug. 2023, doi: 10.3390/app13158798.

[12] P. Vishnuram *et al.*, "A comprehensive review on EV power converter topologies charger types infrastructure and communication techniques," *Front Energy Res*, vol. 11, Feb. 2023, doi: 10.3389/fenrg.2023.1103093.

[13] M. Thirumeni and D. Thangavelusamy, "Performance analysis of PI and SMC controlled zeta converter," *International Journal of Recent Technology and Engineering*, vol. 8, no. 3, pp. 8700–8706, Sep. 2019, doi: 10.35940/ijrte.C5242.098319.

[14] M. Memon, H. Memon, S. M. Jiskani, F. Umer, A. M. Soomro, and A. A. Ali Sahito, "Performance Improvement of Buck Converter with Sliding Mode Controller," *Indian J Sci Technol*, vol. 11, no. 46, pp. 1–7, Dec. 2017, doi: 10.17485/ijst/2018/v11i46/139717.

[15] S. Markkassery, A. Saradagi, A. D. Mahindrakar, N. Lakshminarasamma, and R. Pasumarthy, "Modeling, Design and Control of Non-isolated Single-Input Multi-Output Zeta-Buck-Boost Converter," in *IEEE Transactions on Industry Applications*, Institute of Electrical and Electronics Engineers Inc., Jul. 2020, pp. 3904–3918. doi: 10.1109/TIA.2020.2984190.

[16] A. J. Injeti and P. K. Das, "Analysis of high efficiency single-input triple-outputs dc-dc converter with coupled inductor," in *Proceedings of the 7th International Conference on Electrical Energy Systems, ICEES 2021*, Institute of Electrical and Electronics Engineers Inc., Feb. 2021, pp. 9–14. doi: 10.1109/ICEES51510.2021.9383748.

[17] S. K. Ramu *et al.*, "A Novel High-Efficiency Multiple Output Single Input Step-Up Converter with Integration of Luo Network for Electric Vehicle Applications," *International Transactions on Electrical Energy Systems*, vol. 2022, 2022, doi: 10.1155/2022/2880240.

[18] K. A. Mahafzah, M. A. Obeidat, A. Q. Al-Shetwi, and T. S. Ustun, "A Novel Synchronized Multiple Output DC-DC Converter Based on Hybrid Flyback-Cuk Topologies," *Batteries*, vol. 8, no. 8, Aug. 2022, doi: 10.3390/batteries8080093.

[19] P. Chandran, K. Mylsamy, and P. S. Umapathy, "Analytical evaluation of single-input dual-output based integrated luo-buck converter for BLDC motor," *IET Power Electronics*, vol. 16, no. 6, pp. 937–947, May 2023, doi: 10.1049/pel2.12441.

[20] "Fundamentals of Power Electronics. Second Edition." [Online]. Available: http://site.ebrary.com/lib/nankai/Doc?id=10067440&page=1

[21] S. Sankara Kumar and K. Ramash Kumar, "Design of Single Input Dual Output DC-DC Converter for Electric Vehicle Application," *Math Probl Eng*, vol. 2023, 2023, doi: 10.1155/2023/3536608.

[22] L. Zhang, Y. Sun, T. Luo, and Q. Wan, "Sliding-mode control of single input multiple output DC-DC converter," *Review of Scientific Instruments*, vol. 87, no. 10, Oct. 2016, doi: 10.1063/1.4963694.

[23] M. Agostinelli, R. Priewasser, S. Marsili, and M. Huemer, "Constant switching frequency techniques for sliding mode control in DC-DC converters."